Preprints (www.preprints.org) | NOT PEER-REVIEWED | Posted: 15 December 2016 doi:10.20944/preprints201612.0082.v1

Article

The Effect and Mechanism of Transdermal Penetration Enhancement of Fu's Cupping Therapy: A New Physical Penetration Technology for Transdermal Administration with TCM Characteristics

Wei-Jie Xie [1,2], Yong-Ping Zhang [1,*], Jian Xu [1], Xiao-Bo Sun [2], Fang-Fang Yang [1]

[1] School of Pharmacy, Guiyang College of Traditional Chinese Medicine, No. 50 Shidong Road, Guiyang 550002, China.

[2] Institute of Medicinal Plant Development, Chinese Academy of Medical Sciences & Peking Union Medical College, Beijing 100193, China.

Correspondence: zgygpg@126.com Or xwjginseng@126.com. Telephone: 0851-5652056.

Abstract

Background: in this paper, a new physical penetration technology for transdermal administration with traditional Chinese medicine (TCM) characteristics - Fu's cupping therapy (FCT) - was established and studied by in-vitro and in-vivo experiments; the penetration effect and mechanism of FCT physical penetration technology (FCT-PPT) was preliminarily discussed.

Method: Indomethacin (IM) as a model drug，by transdermal in vitro tests the establishment of the high，medium and low reference were finished as the chemical permeation system；chemical penetration enhancers and iontophoresis as a reference，the percutaneous penetration effect of FCT for IM patch was evaluated with 7 species diffusion kinetics model and in vitro drug distribution；naproxen as an internal standard，using UPLC-MS/MS technology，the IM quantitative analysis method in vivo was established，and pharmacokinetic parameters (AUC0-t，AUC0-∞，AUMC0-t，AUMC0-∞, Cmax and MRT) as indicators were used evaluate to FCT penetration role in vivo；in the same time，the group used 3K factorial design to study joint synergistic penetration effect on FCT and chemical penetration enhancers (CPEs)；by SEM and TEM，the skin micro and ultrastructural changes of the stratum corneum (SC) surface were observed, to explore pay tank penetration mechanism.

Results: In vitro and in-vivo skin permeation experiments revealed that both the total cumulative percutaneous amount and in-vivo percutaneous absorption amount (AUC and AUMC) of indomethacin that permeated SD mouse skin using FCT techniques were greater than the amount observed using CPE and iontophoresis: Firstly, in contrast to the control group, the indomethacin percutaneous rate (PR) of the FCT lower group (FCTL) was 35.52%, and the enhancement ratio (ER) at 9h was 1.76X, which was roughly equivalent to the penetration enhancing effect of the CPEs and iontophoresis; secondly, the indomethacin PR of the FCT middle (FCTM) group and the FCT high intensity group (FCTH) were

 doi:10.20944/preprints201612.0082.v1

respectively 47.36% and 54.58%, ER at 9h were separately 3.58X and 8.39X; thirdly, pharmacokinetic studies showed that in-vivo indomethacin percutaneous absorption of the FCTs was higher than that of the control group, that of the FCTM group was slightly higher than that of the CPEs group, and that of the FCTM group was significantly higher than that of the others. Meanwhile, the variance analysis indicated that the combination of the FCT penetration enhancement method and the CPE method had beneficial effects in penetration enhancing of the skin: the significance level of the CPE method was 0.0004, which was apparently lower than the 0.001, meaning the difference was markedly significant; the significance level of the FCT was under 0.0001, its difference markedly significant; and the significance level of factor interaction A×B was lower than 0.0001, indicating that its difference of the synergism was markedly significant. Moreover, SEM and TEM images showed that the SC surfaces of SD rats treaded with FCT-PPT was damaged, and hard to observe the complete surface structure with its SC pores growing bigger and its special "brick structure" becoming looser, indicating that it broke the barrier function of skin, which revealed potentially a major route of skin penetration. Conclusion: FCT, as percutaneous penetration new technologies, has penetration effects significantly, with Chinese characteristics and highly clinical value, worth promoting development.

Keywords: transdermal physical penetration technology; Fu's Cupping Therapy; pharmacokinetics; SEM; TEM; stratum corneum; mechanism

---

Background

During the past several decades, much work has been done to overcome the skin barrier for drug penetration and increase the number of drugs available for transdermal administration, largely deriving from the SC [1-6], which includes mainly the develop of chemical penetration enhancement, physical enhancement and biochemical enhancement methods for transdermal drug delivery, such commonly known as CPEs [1, 7], sonophoresis [8, 9], iontophoresis [1, 10, 11]and microneedle [3, 10-12]. However, to date, the transdermal delivery for most drugs remains a significant challenge due to low permeation rates [10], in particular larger molecular weight drugs。

Cupping therapy is one of the five TCM therapies (medicine, acupuncture, moxibustion, massage and cupping), the earliest ancient records about cupping therapy can be traced back to Prescriptions of Fifty-two Diseases, during the period of the Tang Dynasty, there were documents about the treatment of diseases using "horn cup" (made of ox horn). Fu' Cupping Therapy (demonstrated as Fig.1and Fig.2), marking the comprehensive modernization of innovation and

Preprints (www.preprints.org) | NOT PEER-REVIEWED | Posted: 15 December 2016 doi:10.20944/preprints201612.0082.v1

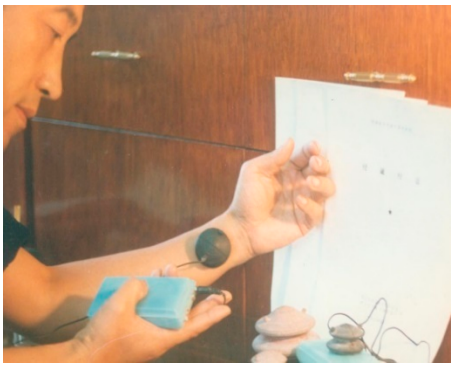

Fig.1 Example of FCT treatment on human skin

Fig.2 Fu's cupping made of white rubber

development of TCM cupping therapy, encloses and creates a confined space between the body skin (or mucosa) and the walls of cup through FCT effect, namely forming a confined space between the body skin (or mucosa) within the FCT treating skin area and the walls of cup, which shapes and serves as an artificial environment of FCT producing various stimulating effects on human skin and subcutaneous structure. And multiple physical, chemical and biological effect parameters within the cup cavity, such as pressure, temperature, and amounts of O_2, CO_2, can be observed and regulated through its observation slot and regulation slot on the cup respectively. Since the cup cavity with small size is constructed artificially that presses on the body, it is called and referred to as "the artificial near-body microenvironment full regulation therapy", namely the theory of "Generalized Meridian – Three Fields and Two Cavities–Gap", which all are part of TCM theories. And FCT's creating several effects on human body as a TCM treatment, especially Skin, have been revealed via modern researches. Among them, several aspects may account for support and interpret this idea of FCT being used as a method of drug enhanced skin penetration.

Based on the above, we focused on the preliminary exploration of utilizing FCT and creating a new physical technology for transdermal administration with TCM characteristics. In our work, 1-(4-chlorobenzoyl)-5-methoxy-2-methylindol-3-ylacetic acid (indomethacin, a model drug) hydrophilic gel patch [13, 14] was prepared as the preparations for transdermal administration. Firstly, compared with CPEs (including 3%Azone and 5%Azone) and iontophoresis, the penetration enhancement effects of FCT (divided into three groups: FCTL, FCTM and FCTH) on indomethacin hydrophilic gel patches were evaluated through the in-vitro and in-vivo transdermal penetration enhancement tests，in which in-vitro transdermal parameters and in-vivo pharmacokinetic parameters were used as the detection indexes. Posteriorly, the synergism between FCT physical penetration technology and chemical penetration enhancers, concerned about those various ratios of CPEs, in transdermal enhancement were investigated initially, utilizing the 3^K factorial design and ultra-performance liquid chromatography-tandem mass spectrometry (UPLC-MS/MS) technologies. Furthermore, Skin treated with chemical penetration enhancers, iontophoresis and the FCT, obtained from in vitro skin penetration studies, was examined via using scanning electron microscope (SEM) [15, 16] and transmission electron microscopy (TEM)[5, 9, 15-20] to investigate the effect of FCT-PPTs on ultrastructural changes of the skin, especially its SC, and to evaluate tentatively and preliminarily the mechanism by which FCT enhances skin penetration.

Preprints (www.preprints.org) | NOT PEER-REVIEWED | Posted: 15 December 2016 doi:10.20944/preprints201612.0082.v1

Methods

Materials

Indomethacin and naproxen references (purity > 99.9%, determined by HPLC) were obtained from National Institutes for Food and Drug Control. HPLC grade Acetonitrile, methanol and formic acid were all obtained from Tedia Company Incorporation (Fairfield, USA). Double distilled 4umulativ water was prepared through a Milli-Q water purification system (Millipore, USA). Indomethacin hydrophilic gel patches were prepared and supplied by Preparation Laboratory of Guiyang College of Traditional Chinese Medicine. Hydrophilic gel matrix materials, used to prepare indomethacin patches, were purchased from Shanghai Ye source Biotechnology Co., Ltd. Sprague-Dawley (SD) rates of SPF grade, weighing 320 to 350 grams (g), were supplied by the Experimental Animal Center of Third Military Medical University (Chongqing, Chin*a).*

Preparation of indomethacin patches

By screening and optimization， prescription of indomethacin matrix were identified; its composition was PVA of 17.350g, gelatin of 9.999g, PVP of 6.260g, CMC-Na of 8.140g, carbomer-940 of 3.000g, glycerol of 12.880g, propylene glycol of 12.880g, triethanolamine of 4.200g.

And the preparation process of matrix patches was as follows: firstly, PVA and gelatin weighed in prescription were properly swollen in the water overnight, heated by a water bath heater and then prepared as the mixed gel solution A (MGSA); secondly, PVPK-30, CMC-Na and carbomer-940 were weighed, mixed, swollen, dissolved, heated and prepared as the mixed gel solution B (MGSB); thirdly, after the weighing and mixing of glycerol, propylene glycol, triethanolamine, model drugs were added and stirred until these drugs were completely dissolved as the mixed gel solution C (MGSB); fourthly, the MGSB and MGSC were added in the solution A correspondingly, stirred while being added, and the water was added until the all solution weighs 600g, evenly stirred, and deposited to remove the air bubbles; in the end, the final MGS was quantitatively poured into a rubber ring attaching to blank matric backings (as long as 7 cm in diameter), extended and frozen for 2h, dried in natural conditions, until a total of 30 patches were formed with the same uniform, thickness and unified colors, and the dosage per patch was 12.5mg.

Standard operation of FCT penetration enhancement

According to TCM theory, the influencing factors associated with FCT mainly comprise cupping method, cupping therapy pressure and time. Therefore, in our research various Fu's cuppings of size (Fig.3) were designed, fabricated and used to control the pressure of cupping therapy and regulate the levels of stimulation to human body. And the No.2, No.3 and No.4 cups pressure regulations were selected from them and the inner air was removed off through the opening on Fu's Cupping using a syringe to create a negative pressure environment (Fig.4). Moreover, diverse cupping operation follows TCM clinical operation procedure.

Retaining cupping, keeps the cup on the part to be cupped or retaining cup to follow the meridians, generally in a duration of 5～15min, preferably in 7min, with the function of warming meridians, also referred to as "warming cupping". Shaking cupping, or spinning cupping: cup on the skin, then rhythmically shake and pull cup on the skin; gently shake the

Preprints (www.preprints.org) | NOT PEER-REVIEWED | Posted: 15 December 2016 doi:10.20944/preprints201612.0082.v1

cup, the speed should not be too fast, shake at an appropriate angle, and operate once every 2s.
Moving cupping, also known as slipping or scraping cupping, often applied the larger part of lesions or muscular part, namely apply a layer of massage oil or glycerin on such part, press the cup on skin with the left hand, make it tightly secured, pull the cup with the right hand at one direction to make it slip along the meridians, until the skin flushes.
Based on this procedure, experiments of FCT penetration enhancement were divided into three groups: the high, middle and low intensity group of FCT penetration enhancement，abbreviated as FCTL，FCTM and FCTH，were formed as shown in Table 1.

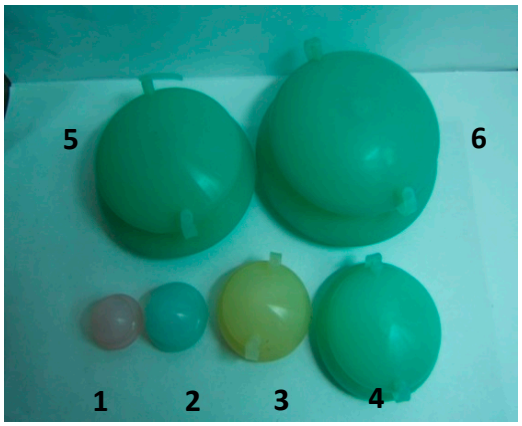

Fig.3 Images of No. 1～6 Fu's cupping

Fig.4 "Vacuum" operation of Fu's cupping

Table 1 Treatment condition parameters of FCT transdermal penetration enhancement

FCT groups	Cupping operation	Cupping No.	time
FCTL	Retaining cupping	2	6min
FCTM	Shaking cupping	3	11min
FCTH	Moving cupping	4	15min

In-vitro transdermal penetration enhancement study

Quantitative methods

Agilent 1260 high-performance liquid chromatograph system (US Agilent) was exploited for quantification with the VWD detector and a C18 chromatographic column (5μm, 250×4.6mm, Diamonsil, Beijing, China). At chromatographic conditions, the mobile phase was composed of a mixture of acetonitrile-0.1% aqueous phosphoric acid (60:40, v/v). And the analysis was carried out at a flow rate of 1 ml/min with the detection wavelength set at 228 nm at 35℃.

In-vitro transdermal test

The Franz in-vitro transdermal diffusion device [15, 20] was used to carry out in vitro transdermal experiments [2] with the volume of receiving pool (V, 7.0ml) and the contact area (A, 2.92cm^2), divided into 8 groups, i.e.: the blank group, the 3%Azone group, the 5%Azone group, the 3%Azone-5%Mint oil group (dualistic enhancers, namely DCPEs group), the iontophoresis group, the FCT groups, processed as per the requirements of each group. And patches were used to administer drugs.

First of all, 20% ethanol PBS solution were used as receiver solution, and the skins of SD rats were used as percutaneous medium; after that, the skin was tightly fit to the patches and fixed

Preprints (www.preprints.org) | NOT PEER-REVIEWED | Posted: 15 December 2016 doi:10.20944/preprints201612.0082.v1

on the diffusion pool. Secondly, the receiver solution and its watery environment were completely adjusted to the constant temperature at 37℃±1℃, electromagnetically stirred at the constant speed of 320r/min; at last, we immediately filled up the control receiver solution after sampling and fully withdrawing at 3h, 6h, 9h, 12h, 16 h, 24h, 30h and 36h respectively. After such treatment, the sample were determined analyze the drug concentration (C, μg/ml) at each time point, and total cumulative penetration amount at all points and the cumulative penetration amount per unit area (Q_A, μg/cm^2) were calculated as shown in Equation 1.

$$Q_A = \frac{\sum_{i=1}^{n} Ci \times Vi}{A} \qquad \text{(Equation 1)}$$

Index detection

According to the in-vitro cumulative transdermal penetration amount [18] of indomethacin (Q, μg) at each point; the ratio of cumulative transdermal penetration amount to total dosage of indomethacin was calculated, namely the cumulative penetration percentage (Q%); and the "1-Q%" denoted the remaining dosage percentage of matrix at different time points. The cumulative penetration percentage (Q %) was used as the y-coordinate and the time (t) was used as the x-coordinate to draw out the Q%-time curve of indomethacin in-vitro percutaneous diffusion tests (Fig.5 and Fig.6). Compared with the blank (or control) group, Q_{A9}, Q_{A24} at 9h and 24h of each group and the enhancement ratio (ER) at two time points were calculated as shown in Table 2.

After the completion of experiments, the matrix patch and skin were removed and cut into pieces, and then extracted for 90min using 50ml methanol and heating reflux, extracted once; and then the indomethacin residual in the matrix patch and in skin with each extraction solution was detected to obtain the indomethacin distribution in paste, skin and receiver solution was shown as Fig.7.

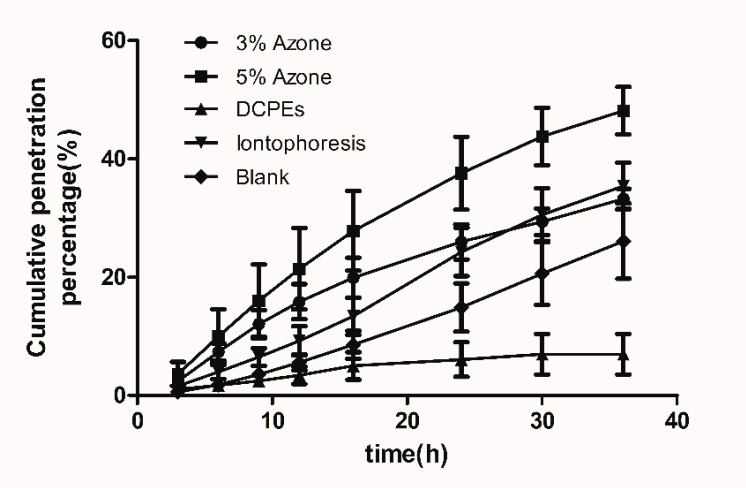

Fig.5 Q%-time curve of in-vitro percutaneous tests on the reference groups (n=6): the 3% azone-CPE group (●) , the 5% azone-CPE group (■), the DCPEs group (▲), the iontophoresie group (▼), the blank group (◆).

Preprints (www.preprints.org) | NOT PEER-REVIEWED | Posted: 15 December 2016 doi:10.20944/preprints201612.0082.v1

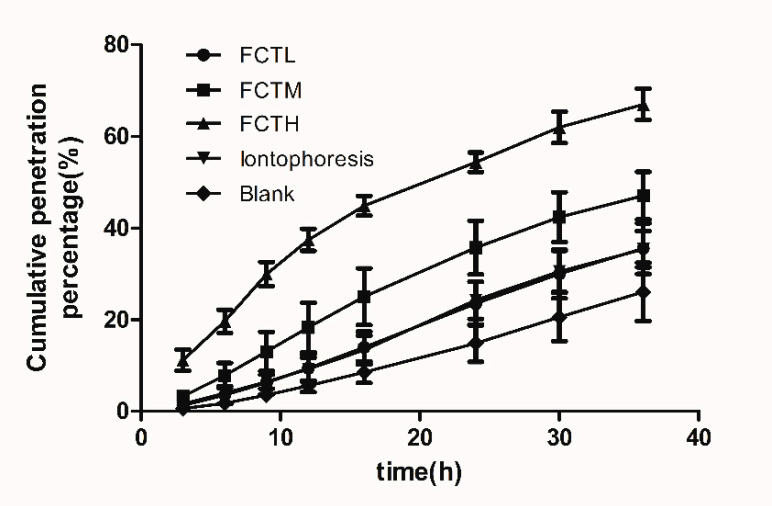

Fig.6 Q%-time curves of in-vitro percutaneous tests on the FCT penetration enhancement groups (n=6): the FCTL group (●) , the FCTM group (■), the FCTH group (▲), the iontophoresie group (▼), the blank group (◆).

Table 2 In-vitro percutaneous test data of each group (Mean ± SD，n=6)

Group	Q_{A9} (μg/cm²)	Q_{A24} (μg/cm²)	ER_9	ER_{24}
Blank	23.72±5.60	98.98±12.82	1.06±0.26	1.11±0.30
3% Azone	70.72±17.22	150.4±22.86	2.98±1.20	1.52±0.27
5% Azone	62.97±27.53	146.02±34.86	2.65±1.16	1.48±0.35
DCPEs	9.82±3.66	27.34±5.35	0.36±0.21	0.23±0.12
Iontophoresis	42.17±12.64	153.89±33.99	1.78±0.53	1.55±0.34
FCTL	41.79±17.72	156.21±35.56	1.76±0.82	1.58±0.39
FCTM	84.88±26.37	232.13±35.04	3.58±1.11	2.35±0.35
FCTH	199.08±14.48	361.54±14.73	8.39±0.61	3.65±0.15

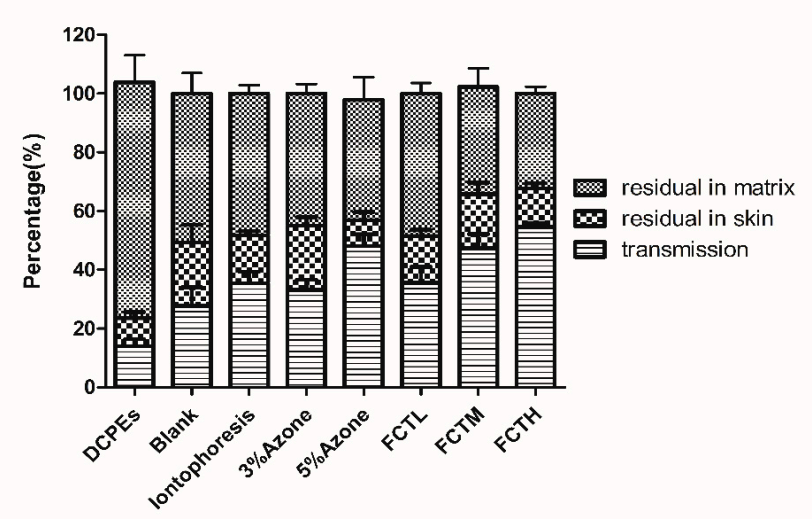

Fig.7 Illustrative diagram of in-vitro transdermal drugs distribution: the indomethacin residual in the matrix patch (▒), the indomethacin residual in skin (▩), the transmission indomethacin (▤).

Preprints (www.preprints.org) | NOT PEER-REVIEWED | Posted: 15 December 2016 doi:10.20944/preprints201612.0082.v1

In-vivo transdermal penetration enhancement

Quantitative method

The analysis was performed on a WATERS Xevo TQ UPLC-MS/MS system (Waters, USA), where the chromatographic column of ACQUITY UPLC Shield RP (C18, 1.7μm, 2.1×50mm, Waters, USA) and the mobile phase of the acetonitrile-0.05% formic acid was used to enables complete separation of target components separate under the gradient elution (Table 3). Simultaneously, the total ion chromatograms(TIC) and quantitative data were recorded and processed by using an electrospray ion source [21] under the mass spectrum conditions: the ion source temperature (150℃), the capillary voltage (3.0KV), the first cone voltage (40V); the desolventized gas (DG, N_2), the temperature of DG (550℃), the flow of DG (750l/h), the cone gas flow (50l/h); the collision gas (CG, Ar), the collision gas flow rate (0.15ml/min); the indomethacin quantitative ion reaction: Parent(M/Z)356.1198→Daughter(M/Z)111.9691＋Daughter(M/Z)138.9997; the quantification for naproxen (an internal standard): Parent(M/Z) 231.1855→ Daughter(M/Z) 185.0841, seeing Table 4 for the ion peak spectrum conditions.

Table 3 Gradient change of the mobile phase

Time	Flow rate (m1/min)	Aqueous phase (%)	Organic phase (%)	Curve
0.0	0.3	64.0	36.0	6
1.0	0.3	54.0	46.0	6
2.1	0.3	48.0	52.0	6
4.5	0.3	25.0	75.0	6
5.0	0.3	10.0	90.0	6
6.0	0.3	10.0	90.0	6
6.5	0.3	64.0	36.0	6
7.5	64.0	36.0	38.0	6

Table 4 Mass spectrum conditions of quantitative ion peak

Compound	Parent(M/Z)	Daughter(M/Z)	Dwell(s)	Cone(V)	Collision(V)
Indomietacin	358.1198	138.9997	0.49	18	20
Indomietacin	358.1198	111.9691	0.49	16	48
Naproxen	231.1855	185.0841	0.49	16	14

In-vivo percutaneous penetration enhancement test

SD rates were chosen and randomly divided into 5 groups, i.e.: the control group, the FCTM group, the FCTL group, the CPE-3%azone group and the CPE-5%azone group. After the intraperitoneal injection and anesthesia using 10% urethane, rats were unhaired and the shu-back points were marked and treated as per the requirement of each group; in addition, the work area 3.14cm^2 were selected within the marked part of skin, and used to administer drugs with the patches dosage of 2.0mg/rat; the 3%azone patches were delivered to the chemical enhancer group, the none-enhancer patches were used to the control group, and the patches were used to administer drugs after cupping therapy treating in the FCT group.

The capillary (the sodium treatment was done using heparin) with diameter of 1.0mm was

Preprints (www.preprints.org) | NOT PEER-REVIEWED | Posted: 15 December 2016 doi:10.20944/preprints201612.0082.v1

used to take 0.5ml blood from the venous plexus under the eye sockets of rats; the whole blood samples were taken at 1h, 3h, 6h, 9h, 12h, 16h, 20h, 24h, 28h, 36h and 48h respectively, then placed into anticoagulation EP. And plasma was prepared by centrifugation. 100 μl of rat plasma were mixed with 700 μg of internal standard, and 1ml of ethyl acetate was added into it to extract. The mixture was vortexed for 10 minutes and then centrifuged at 12,000 rpm for 13min in a centrifuge at 10℃. Then 800 μl of supernatant raffinate was be transferred to into a nitrogen blowing concentrator (Tianjin Automatic Science Instrument Co., Ltd, Tianjin, China) to evaporate, until turned into a residue. The residue was dissolved with 0.5ml of acetonitrile, then used to detect via the UPLC-MS/MS system.

Concentration-time curve of each group

According to the blood concentration (C, ng/l) of each group, the concentration (C, ng/l)-time (t, h) curve of each group was drawn. And in contrast, the findings showed that the C-t curve of FCTM group was significantly higher than that of any other group, while the concentration-time curve of FCTL group was slightly higher than that of the chemical penetration enhancer group (Fig.8).

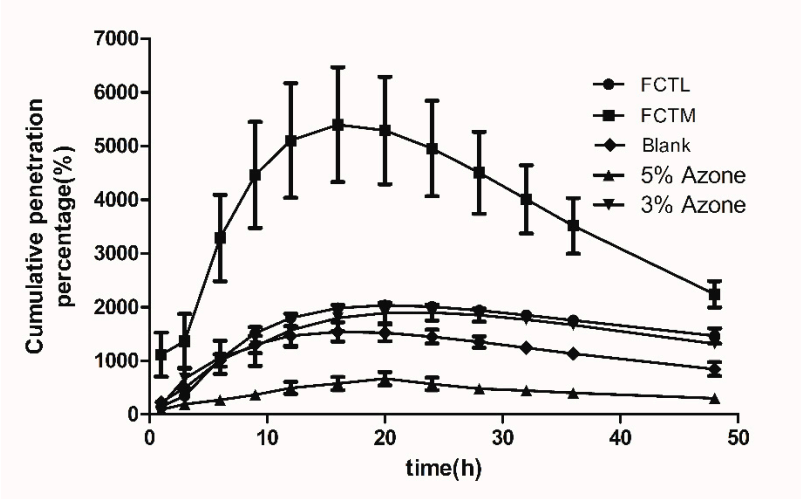

Fig.8 The concentration-time curve of each groups: the FCTL group (●) , the FCTM group (■), the blank group (◆), the 5% azone-CPE group (▲), the 3% azone-CPE group (▼).

Penetration enhancement synergism study

The synergism of FCT penetration enhancement and CPE was examined and using a 3^K factorial design: the chemical enhancer was used as "Method A" and FCT penetration enhancement was used as "Method B"; the levels were divided into 3 grades; 9 groups of experiments were carried out and there were 3 repeated experiments in each group, meaning a total of 27 groups of experiments were carried out. After detecting and analyzing with the UPLC-MS/MS system, the areas ($AUC_{(0-t)}$ and $AUC_{(0-\infty)}$) under the curve in the compartment model parameters and the $AUMC_{(0-t)}$, $AUMC_{(0-\infty)}$ and C_{max} under the moment curve in the statistical moment model were used as the evaluation indexes for the penetration enhancement synergistic effect, denoted as Y_1, Y_2, Y_3, Y_4 and Y_5 respectively; the normalization value (Y) of all indexes was calculated according to this formula: $Y = Y_1/Y_{1max} + Y_2/Y_{2max} + Y_3/Y_{3max} + Y_4/Y_{4max} + Y_5/Y_{5max}$, shown as Table 5.

Preprints (www.preprints.org) | NOT PEER-REVIEWED | Posted: 15 December 2016 doi:10.20944/preprints201612.0082.v1

Table 5 3^K factorial design experiments and results (mean，n=3)

No.	Arrangement		Indexes					
	A	B	$AUC_{(0-t)}$	$AUC_{(0-\infty)}$	$AUMC_{(0-t)}$	$AUMC_{(0-\infty)}$	C_{max}	Y
1	A2	B2	111719.3	210014.8	2838513.9	13136654.4	3804.7	3.0729
2	A3	B2	180273.1	232490.9	4164900.5	11384695.4	5071.9	3.7996
3	A3	B1	23020.6	37342.7	526321.8	2601184.1	783.0	0.5936
4	A2	B3	183710.8	246637.1	4072945.2	11759021.4	7699.2	4.1762
5	A1	B2	78319.7	168943.8	1992035.2	17113618.1	2547.5	2.6779
6	A3	B3	213673.0	287876.3	4611002.6	12129243.6	7848.5	4.6126
7	A2	B2	120784.2	206597.8	2982561.4	9664642.7	3749.7	2.9244
8	A3	B2	138878.5	222301.1	3203710.7	10611719.3	4571.1	3.2620
9	A3	B3	216275.8	265210.8	4522867.7	10476852.1	8332.3	4.4871
10	A1	B2	75333.4	155938.5	1955883.4	14172778.8	2654.9	2.4520
11	A2	B1	78904.7	130605.9	1865553.4	10963153.6	2680.9	2.1763
12	A3	B1	21086.6	30890.2	534802.3	1450696.0	781.7	0.4968
13	A3	B1	22260.1	31662.5	539603.5	1243886.5	778.5	0.4934
14	A2	B3	167116.1	236699.1	3990846.2	11035754.6	6723.3	3.8905
15	A2	B3	176350.6	219040.3	3875846.5	8132089.2	6972.3	3.7062
16	A3	B2	139788.1	233712.5	3275263.6	11562142.3	4694.3	3.3914
17	A1	B2	76484.1	148867.2	2014480.7	8270573.6	2585.1	2.0923
18	A2	B1	66105.0	138918.8	1837867.3	6682340.1	2330.6	1.8491
19	A1	B1	56226.6	70071.4	1479349.1	2427650.7	2296.3	1.2343
20	A1	B3	184695.5	257778.8	4263475.2	9408589.7	7276.9	4.0736
21	A1	B3	205118.5	262470.6	4028318.3	10487269.7	6175.2	4.0656
22	A3	B3	218339.7	260469.6	4459896.9	10219832.9	8483.0	4.4692
23	A2	B2	138911.4	201867.2	3177125.0	9951217.1	4198.8	3.1029
24	A2	B1	68813.4	122355.1	1846695.4	6065224.4	2398.4	1.7778
25	A1	B3	159918.6	225284.1	3750856.5	10929334.3	5940.6	3.6674
26	A1	B1	55597.1	70376.0	1374052.5	1969217.5	2621.4	1.2212
27	A1	B1	56396.7	68021.0	1309444.7	2121255.4	2436.0	1.1897

Skin structure study by SEM and TEM

Grouping and treatment of animals

SD rats were randomly divided into 6 groups, i.e.: the control group, the FCTL, the FCTM, the FCT group, the CPE-3%azone, the CPE-5%azone. Then an electric knife was used to dehair on the abdomen and back skin of SD rats, and after the dehairing and cleaning with warm water the medical absorbent cotton was used to dry the skin, which was reserved for use after observing the surface skin under the magnifying glass without any damage. Furthermore, the FCT groups were treated for some time using the FCT standard operation; in the CPE groups, the patches with different enhancers were stuck to the skin and treated for 12h; the control group was treated using the patches without any enhancer for 12h.

Sample preparation and observation

After these animals were treated using the said method, the skin samples were cut in vivo from the treated parts, 4% paraformaldehyde solution was firstly used to fix, then 2.5%

Preprints (www.preprints.org) | NOT PEER-REVIEWED | Posted: 15 December 2016 doi:10.20944/preprints201612.0082.v1

glutaraldehyde was used to solidify, and placed in a refrigerator to preserve and solidify at 2～4℃ for 24h. The 2mm×2mm tissue block was dehydrated, dried and "metal spraying" plating, then the surface structure of skin SC was observed by a JSM-6940 SEM (Hitachi, Japan); after the 1mm×1mm tissue block was rinsed, dehydrated, soaked, embedded and treated in other methods using 0.1mol/LPBS, the ultra-thin sections were prepared and stained, and the SC ultrastructure were observed via a Hitachi-7650 TEM (Hitachi, Japan).

Results

Analysis of in-vitro results

The in-vitro results (Fig.10 and Fig.11) showed that FCT had a significant effect on the transdermal penetration enhancement: Firstly, compared with the control group, the indomethacin percutaneous ratio (Fig.12) of the FCTL group as a result of penetration enhancement was 35.52%, indicating the FCTL (35.52%), the CPE group (33.21%) and iontophoresis group (35.36%) with respect to the effects of penetration enhancement were roughly equivalent, and the enhancement ratio (ER) of the FCTL at 9h was 1.76X of the control group with a significant effect of penetration enhancement (Table 2).Secondly, the indomethacin penetration ratio (Fig.12) of the FCTM, the FCTH was 47.36%, 54.58% respectively, and ERs (Table 2) at 9h were 3.58X, 8.39X respectively of the control, meaning their effects of penetration enhancement were significant and higher than that of the CPE groups and iontophoresis group. Thirdly, the FCTM and FCTH ERs (Table 2) at 24h were 2.35X and 1.76X respectively, slightly higher than that of the CPEs group and iontophoresis group; nevertheless, the decrease of penetration enhancement intensity appearing in late stage might be associated with the recovery of skin barrier function with time, thus the recoverability of skin barrier function after being treated by FCT penetration enhancement needs to be evaluated in the subsequent studies. Besides, it was found that: compared with the control group, the DCPE system of 3% azone-5% mint oil conversely reduced the IM percutaneous ratio, which was only 14.1%, but its ER at 9h was 0.41X, indicating the inhibitory percutaneous effect of the DCPE on indomethacin.

Analysis of in-vivo pharmacokinetic results

According to the concentration-time curves (Fig.13), the single-compartment model and statistical moment model were adopted to analyze pharmacokinetic results under the concentration weight (W=1), and the analysis software Excel and DAS2.0 were combined to calculate and obtain the pharmacokinetic parameters. The curves $AUC_{(0-t)}$ and $AUC_{(0-\infty)}$ in the compartment model parameters and the $AUMC_{(0-t)}$, $AUMC_{(0-\infty)}$ and C_{max} under the curves in the statistical moment model were applied as the in vivo evaluation indexes for comparison and analysis of penetration enhancement effects (Table 6 and Table 7). The findings showed that AUC and AUMC of in-vivo percutaneous absorption as a result of FCT penetration enhancement were higher than that of the control group; AUC and AUMC of the FCTL group were slightly higher than that of the CPE group; the AUC and AUMC of the FCTM group were significantly higher than that of any other group, which indicated that FCT had a facilitating effect on IM transdermal absorption.

Preprints (www.preprints.org) | NOT PEER-REVIEWED | Posted: 15 December 2016 doi:10.20944/preprints201612.0082.v1

Table 6 Pharmacokinetic parameters of the single compartment model (man ± SD，n=5)

Parameters	Units	Blank group	FCTL group	FCTM group	3%Azone group
$t_{1/2}$	h	11.54±2.90	26.983±12.76	12.21±1.435	21.24±2.33
K_e	1/h	0.063±0.014	0.03±.0.013	0.057±0.007	0.033±0.002
$V_{1/F}$	L/kg	4468.073±357.78	7900.616±2567.2	0.002±0.001	0.005±0.001
$AUC_{(0-t)}$	ng/L·h	60657.9±4769.5	76954.5±3456.3	202536.4±34441.9	69717.0±7375.0
$AUC_{(0-\infty)}$	ng/L·h	74052.2±8657.0	140008.4±2478.0	261046.8±41858.0	128452.6±40350.0
K_a	1/h	0.072±0.013	0.11±0.04	0.074±0.003	0.067±0.025
$t_{1/2Ka}$	h	9.837±1.939	7.38±1.27	9.47±0.83	14.08±2.35
T_{lag}	h	1.581±0.058	1.98±0.65	1.55±0.37	1.03±0.42

Table 7 Pharmacokinetic parameters of statistical moment model (mean ± SD，n=5)

Statistical moment	Units	Blank group	FCTL group	FCTM group	3%Azone group
$AUC_{(0-t)}$	ng/L·h	60215.3±2545.7	76863.2±6073.9	198723.21±72277.6	69890.3±10126.1
$AUC_{(0-\infty)}$	ng/L·h	71421.4±9799.5	133223.3±61402.0	266934.83±106453.2	135231.6±23072.1
$AUMC_{(0-t)}$		1389211.5±135642	1974495.4±166810.9	4615582.1±1490332.7	1812179.2±148177.3
$AUMC_{(0-\infty)}$		2298997.6±434956.0	9511822.1±4546771.1	11145184.9±3525715.1	7884625.7±611512 3.2
$MRT_{(0-t)}$	h	22.97±1.973	25.68±0.63	23.52±1.15	26.29±2.09
$MRT_{(0-\infty)}$	h	31.52±3.541	59.61±17.105	40.74±16.00	54.11±16.5
$VRT_{(0-t)}$	h^2	125.58±6.505	142.90±18.23	141.29±5.532	143.50±5.55
$VRT_{(0-\infty)}$	h^2	581.99±619.73	3056.1±4545.21	1111.18±538.547	2671.00±1042.28
$t_{1/2z}$	h	13.76±9.79	30.27±13.23	17.81±7.468	30.59±5.93
T_{max}	h	18.00±5.16	28.00±2.83	19.20±3.38	24.67±8.91
C_{max}	ng/L	2390.89±379.08	2613.09±307.60	7997.04±2153.94	2209.90±548.59

Variance analysis of synergism study

According to the results, the normalization values (Y) of $AUC_{(0-t)}$, $AUC_{(0-\infty)}$, $AUMC_{(0-t)}$, $AUMC_{(0-\infty)}$ and C_{max} was used as the indexes, and the Design-Expert 8.0.5 was operated to make the regression and variance analysis; and A, B and A×B interaction effects were showed by making a three-dimensional (3-D) chart analysis and a visual analysis (Table 8, Fig.14 and Fig.15).

Findings were that: firstly, the variance analysis of regression model ($P< 0.0001$, Table 8) and the multiple correlation coefficient ($R^2 = 0.9856$, Table 8) suggested that this model had a significance, indicating that the model is good; secondly, the significance level of A (CPE) was 0.0004 and the difference was markedly significant, indicating Factor A (CPE) had a markedly significant effect on the experiments; thirdly, the significance level of B (FCT) was under 0.0001 and the difference was markedly significant; if combined with the 3-D chart of subjective effects (Fig.9), it demonstrated that Factor B (FCT) had a markedly significant effect on the indomethacin in-vivo percutaneous absorption. The significance level of factor

Preprints (www.preprints.org) | NOT PEER-REVIEWED | Posted: 15 December 2016 doi:10.20944/preprints201612.0082.v1

interaction A×B (P, Table 8) was beneath 0.0001 and its difference was markedly significant, indicating that A×B interaction has a markedly significant effect on the in-vivo percutaneous absorption of IM; if combined with the A×B interaction visual chart (Fig.10), it demonstrated that the combination of the FCT and CPEs generated a significant synergistic effect (synergism) on the penetration enhancement of indomethacin. And the independent analysis findings of each index were consistent with the analysis results of normalization values.

Table 8 Variance analysis of 3K factorial design

Source	Sum of squares	df	Mean square	F value	P value	Significance
model	43.85	8	5.48	145.05	< 0.0001	***
A-A	0.95	2	0.48	12.62	0.0004	***
B-B	38.43	2	19.21	508.41	< 0.0001	***
A×B	4.47	4	1.12	29.59	< 0.0001	***
pure error	0.68	18	0.04			
Cor total	44.53	26				

Note: * P<0.05 significant difference; ** P<0.01 very significant difference; *** P<0.001 markedly significant difference.

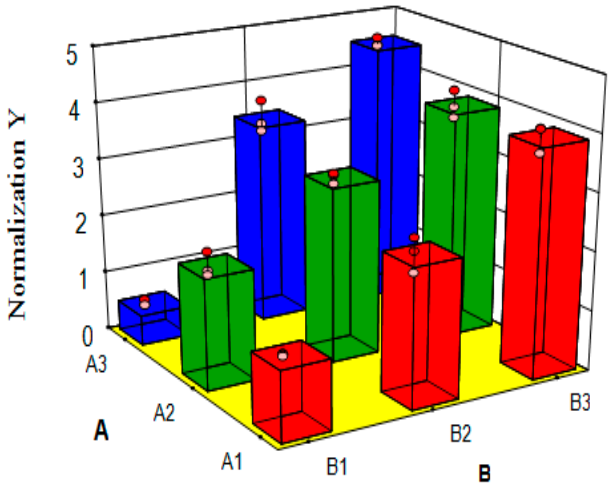

Fig.9 3D image of the Factor A and B subjective effects

Preprints (www.preprints.org) | NOT PEER-REVIEWED | Posted: 15 December 2016 doi:10.20944/preprints201612.0082.v1

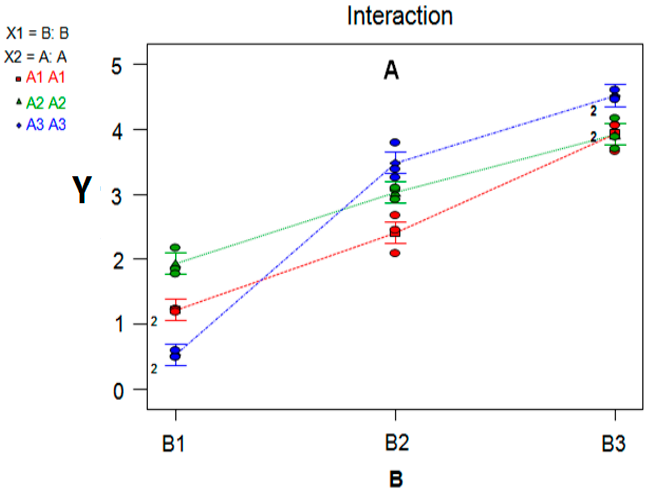

Fig.10 Illustrative diagram of the Factor A×B interaction

Analysis of SEM images

The SEM images were as shown in Fig.11 (A-F). The figures were ×200X with 400×300 pixels, which were reduced to 60.0×70.0mm.The control group images indicated that the SC surface cells of SD rats were flat, relatively regular, and closely spaced with some ridgelines and zigzagging arrangement, as shown in the yellow-arrow part (Fig.11 A).

In comparison with the control group (Fig.11 A), the FCTL (Fig.11 B) and the FCTM (Fig.11 C) images had more cracks, loose and irregular arrangement on the SC surface structure; meanwhile, the SC surface presented the microstructure slices and the skin SC pores grew bigger as shown in the red-circled part; and with the increase of FCT penetration enhancement, the SC structure fissure grew partly bigger as marked in the yellow-arrow part. The SC surface of SD rats in the FCTH (Fig.11 D) was almost completely damaged, hard to observe the complete SC surface structure. These revealed that dense structure of the SC has been damaged to varying degrees by diverse FCTs, which was probably part of the percutaneous penetration mechanism.

Compared with the control group (Fig.11 A), the CPE-3%azone group (Fig. 11E) and the CPE-5%azone group (Fig.11 F) had slightly bumpy wrinkles, relatively loose arrangement and irregular arrangement on the flat surface structure of the SC; with the increase of CPE penetration enhancement, the SC grew bigger as marked in the yellow-arrow part.

By contrast with the FCT groups, the SC surface of SD rats treated by CPEs had internal bumpy wrinkles that were clearly shown in Fig.11 E and Fig.16 F, and had no significant cracks with relatively loose arrangement, but less clearly shown than the FCT group; besides, the SC surface pores didn't grow bigger evidently as marked in the red-circled part.

Furthermore, FCT high intensity group damaged SC and the lower portion of vascular structure (vessels and microangiums) beneath SC was observed as marked in the red-arrowed part (Fig.12), depriving or decreasing its barrier function, and consequently the in-vitro animal skin had cracks after 24h during the in-vitro percutaneous absorption experiments, which made it impossible to go on further percutaneous experiments.

Preprints (www.preprints.org) | NOT PEER-REVIEWED | Posted: 15 December 2016 doi:10.20944/preprints201612.0082.v1

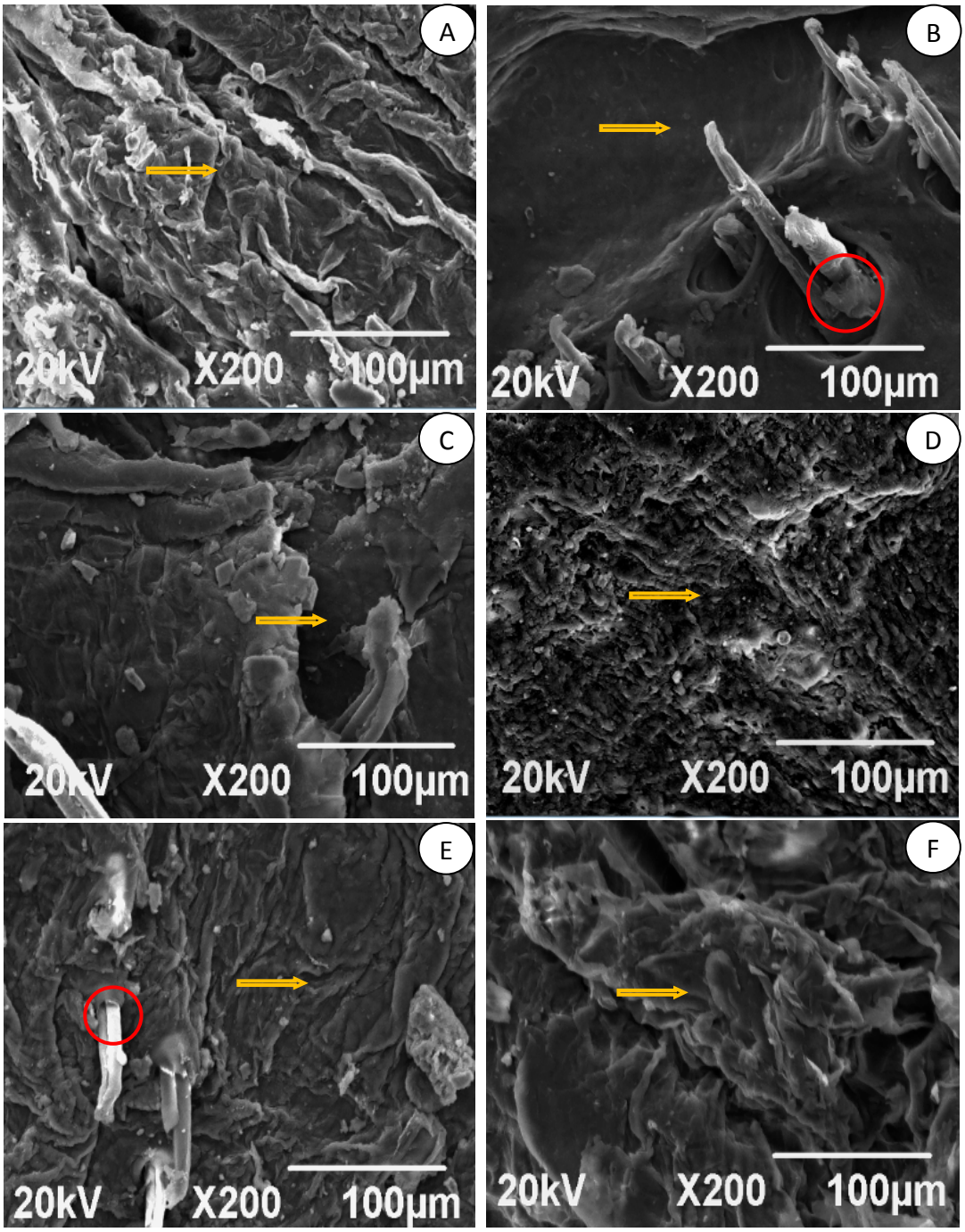

Fig.11 SEM images of SD rat skin SC in each group after the penetration enhancement treatment: the control group (A), the FCTL group (B), the FCTM group (C), the FCTH group (D), the CPE-3%azone group (E), the CPE-5%azone group (F).

Preprints (www.preprints.org) | NOT PEER-REVIEWED | Posted: 15 December 2016 doi:10.20944/preprints201612.0082.v1

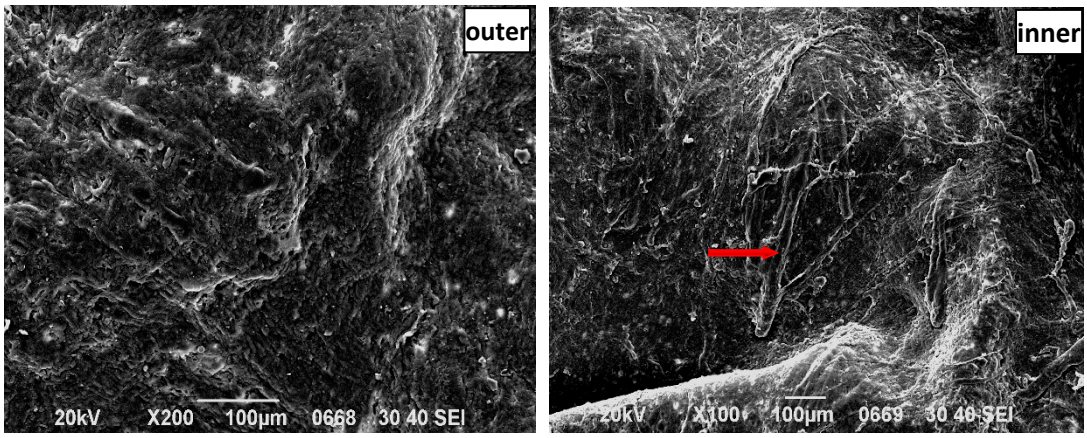

Fig. 12 SEM images of the FCTH group (the outer and inner of SD rat skin).

Analysis of TEM observation images

The control group, FCT low intensity group, FCT middle intensity group, chemical enhancer low intensity group, and chemical enhancer middle intensity group were shown in Fig.13 (A-D) respectively; the 16×3,000X figure was obtained from Hitachi TEM System, the size of which was reduced to 70.0×67.8mm.The control group (Fig.13A) indicates that the keratinocytes SC ultrastructure of normal SD rats had the compact "brick structure", which was regularly and closely arranged, overlaid layer by layer, with lipid composition between the layers that was densely spaced and flat-shaped; it constitutes the complete lipid film with compact structure, low water content and high resistance, which has the function of barrier protection and is considered to be the major obstacle to the transdermal absorption of drugs as indicated in the yellow-arrow position.

Compared with the control group, after the treatment of FCT penetration enhancement as shown in Fig.13B, the "brick structure" from SC became loose, the gap increased, with the irregular arrangement and the lower degree of overlaying, and such changes can reduce the resistance of drugs penetration and increase the transdermal absorption of drugs.

Compared with the control group, the SC ultrastructure after the treatment of chemical penetration enhancer (Fig.13C and Fig.13D) had the loose arrangement, the gap was reduced, but this change was less clear than FCT group, and the intersecting degree of keratinized structure insignificantly reduced as indicated in the yellow-arrowed position.

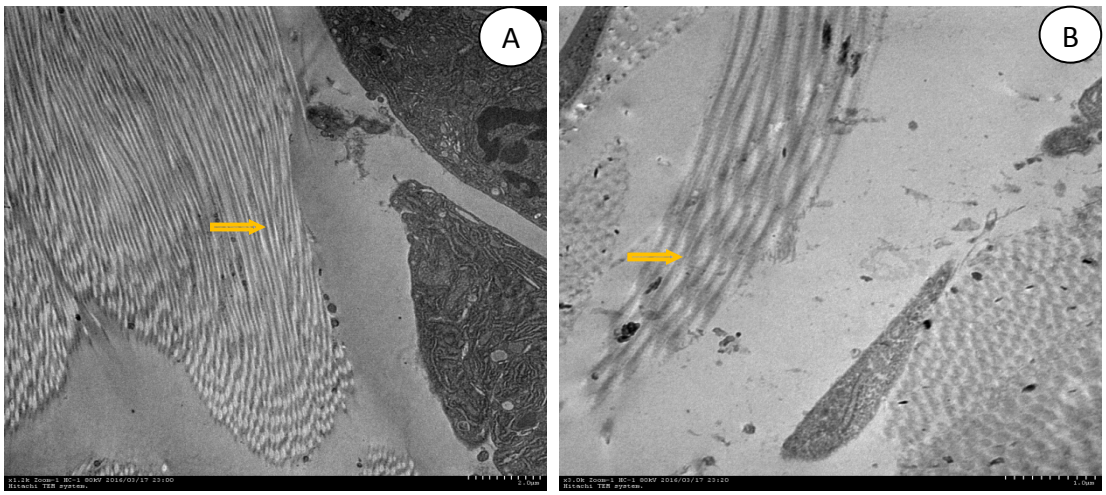

Preprints (www.preprints.org) | NOT PEER-REVIEWED | Posted: 15 December 2016 doi:10.20944/preprints201612.0082.v1

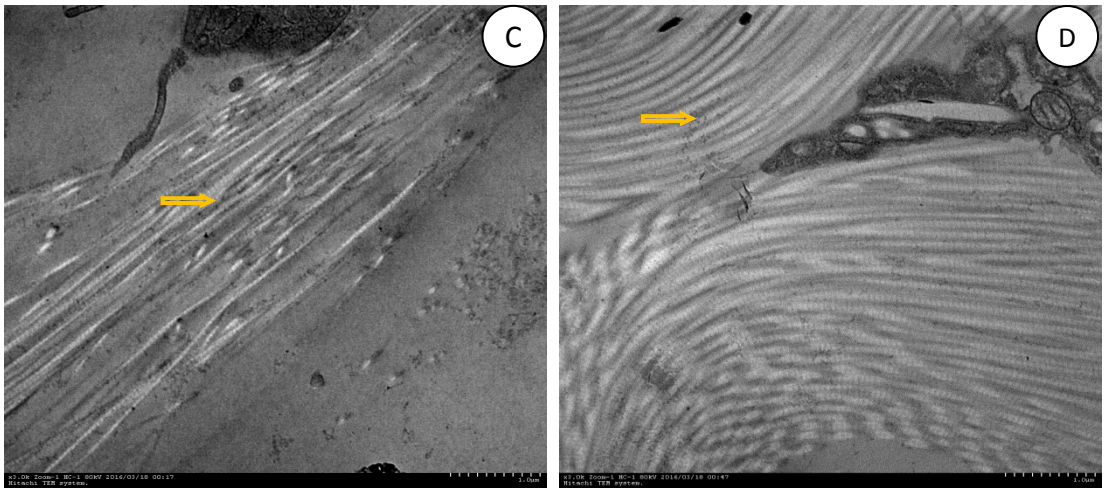

Fig.13 SEM images of rat skin SC in each groups after the penetration enhancement treatment: the control group (A), the FCTL group (B), the CPE-3%azone group (C), the CPE-5%azone group (D).

Discussion

This research attested that as a new physical technology for transdermal administration, FCT can enhance the IM percutaneous absorption through the in-vitro and in-vivo percutaneous experiments; meanwhile, the FCT and CPEs had a markedly synergistic effect on penetration enhancement. SEM and TEM results showed that the SC structure significantly changed after the treatment of penetration enhancement, which reduces the barrier function and increases the percutaneous absorption of drugs; thus it has been verified that the first action mechanism of FCT-PPT is closely interrelated to its physical effects (negative pressure), and it did not involve other action mechanism of percutaneous penetration enhancer.

Firstly, its physical effects, resulting from subatmospheric pressure of FCT, make the fissures, keratinocyte proliferation and acidic liquid secretion evenly scattered on skin epidermis through stimulating effects of heat, force, bioelectricity and other physical factors; secondly, its chemical effects, stemming from changes of chemical substance body and fluids in the body, treat various acute and chronic diseases and play a role in the prevention of diseases and health care by the combined therapy of drug therapy, Chinese herbal medicine and cupping therapy; thirdly, biological effects and other stimulating effects, including bioelectric effect, opening and closing of ion channels (such as Ca^{2+}), have a comprehensive regulation on the whole human body and SC barrier functions through the changes of physical and chemical properties and conditions, neural activities and body fluid metabolism due to the meridian stimulation, angiectasis, blood flow increase, enhanced permeability of partial biofilm system and other effects, resulting in the overall responses as shown in 14~17.

Preprints (www.preprints.org) | NOT PEER-REVIEWED | Posted: 15 December 2016 doi:10.20944/preprints201612.0082.v1

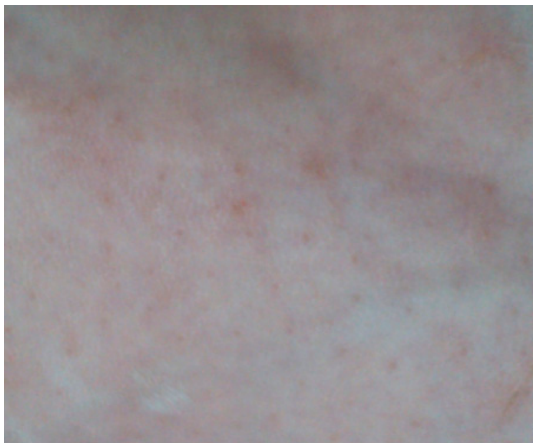

Fig.14 Observation of rabbit's epidermis before FCT treatment

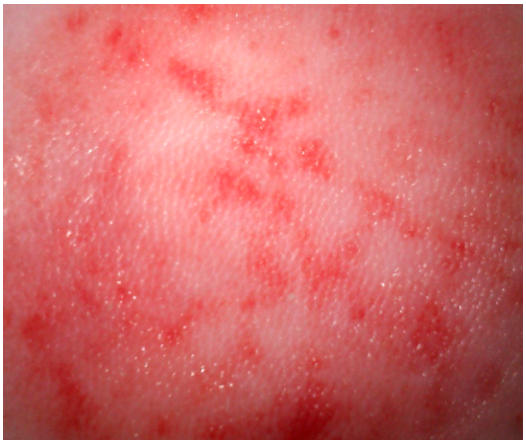

Fig.15 Observation of rabbit's epidermis after FCT treatment

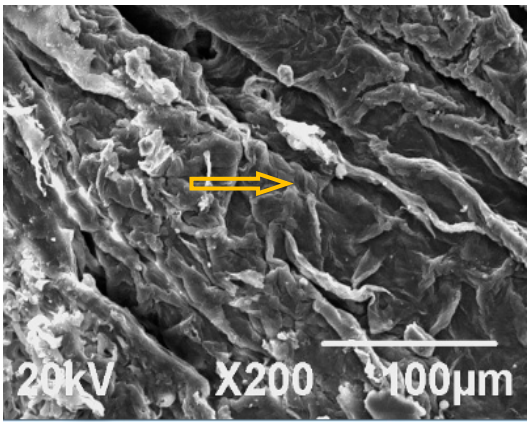

Fig.16 SEM image of FCT penetration enhancement control group

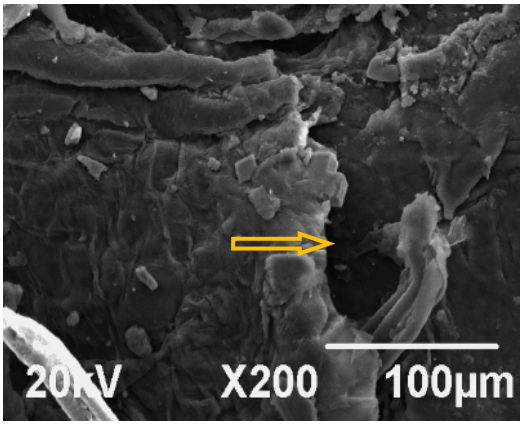

Fig.17 SEM image of FCT penetration enhancement middle intensity group

Conclusion

Therefore, it is considered that FCT as a new physical technology for transdermal administration with TCM characteristics has a significant effect of penetration enhancement as well as a high value of TCM clinical application, which is worthy of being disseminated and developed; its potential mechanism of penetration enhancement and FCT stimulation are closely associated with the change of SC and the biological regulation of skin. But its functional mechanism of penetration enhancement needs to be further researched by fluorescence micro-imaging techniques and various TCM model drugs are required to further validate the effects and features of FCT penetration enhancement.

Declarations

Acknowledgements

We thank Xiaobo Sun and Fang fang Yang for helpful suggestions and advice, as well as key technical support. We also thank the Basic Medicine Laboratory from the Guizhou University of Medical.

Funding

This work was supported by the Project of "A High-level Innovative Talents Training Plan Guizhou" (NO. 20154030) from the Science and Technology Department of Guizhou Province, in China. We express our sincere gratitude to the foundation.

Authors' contributions

WJX and YPZ participated in conceiving the study design, coordinated and performed experiments, analyzed the results, and wrote the manuscript. JX performed experiments, analyzed data, and edited the manuscript. FFY analyzed the in-vivo results and the images of SC. And WJX, YPZ and XBS contributed to the study design and edited the manuscript. All authors read and approved the final manuscript.

Competing interests

The authors declare that they have no competing interests.

Reference

1. Artusi, M., et al., *Effect of chemical enhancers and iontophoresis on thiocolchicoside permeation across rabbit and human skin in vitro.* J Pharm Sci, 2004. 93(10): 2431-8.
2. Bloksgaard, M., et al., *Effect of detergents on the physicochemical properties of skin stratum corneum: a two-photon excitation fluorescence microscopy study.* Int J Cosmet Sci, 2014. 36(1): p. 39-45.
3. Escobar-Chavez, J.J., et al., *Microneedles: a valuable physical enhancer to increase transdermal drug delivery.* J Clin Pharmacol, 2011. 51(7): 964-77.
4. Kendall, M.A., Y.F. Chong, and A. Cock, *The mechanical properties of the skin epidermis in relation to targeted gene and drug delivery.* Biomaterials, 2007. 28(33): 4968-77.
5. Mack Correa, M.C., et al., *Molecular interactions of plant oil components with stratum corneum lipids correlate with clinical measures of skin barrier function.* Exp Dermatol, 2014. 23(1): 39-44.
6. Subongkot, T., et al., *Investigation of the mechanism of enhanced skin penetration by ultradeformable liposomes.* Int J Nanomedicine, 2014. 9: 3539-50.
7. Vineet Mathur, Y.S., Mithun Singh Rajput, *Physical and chemical penetration enhancers in transdermaldrug delivery system.* Asian J Pharm, 2010. 4(3): 173-182.
8. Polat, B.E., et al., *A physical mechanism to explain the delivery of chemical penetration enhancers into skin during transdermal sonophoresis - Insight into the observed synergism.* J Control Release, 2012. 158(2): 250-60.
9. Polat, B.E., et al., *Ultrasound-mediated transdermal drug delivery: mechanisms, scope, and emerging trends.* J Control Release, 2011. 152(3): 330-48.
10. Chen, H., et al., *Iontophoresis-driven penetration of nanovesicles through microneedle-induced skin microchannels for enhancing transdermal delivery of insulin.* J Control Release, 2009. 139(1): 63-72.
11. Yang, Y., H. Kalluri, and A.K. Banga, *Effects of chemical and physical enhancement techniques on transdermal delivery of cyanocobalamin (vitamin B12) in vitro.* Pharmaceutics, 2011. 3(3): 474-84.
12. Bal, S., et al., *In vivovisualization of microneedle conduits in human skin using laser scanning microscopy.* Laser Physics Letters, 2010. 7(3): 242-246.
13. Michael H. Qvist, U.H., Bo Kreilgaard, Flemming Madsen, Lars Hovgaard, and Sven Frokjaer, *Application of Confocal Laser Scanning Microscopy in Characterization of Chemical*

Enhancers in Drug-in-Adhesive Transdermal Patches. AAPS Pharm, 2002. 4(1): 1-8.

14. Patel, R.P., G. Patel, and A. Baria, *Formulation and evaluation of transdermal patch of aceclofenac.* International Journal of Drug Delivery, 2009. 1(1): 41-51.
15. Elnaggar, Y.S., M.A. El-Massik, and O.Y. Abdallah, *Fabrication, appraisal, and transdermal permeation of sildenafil citrate-loaded nanostructured lipid carriers versus solid lipid nanoparticles.* Int J Nanomedicine, 2011. 6: 3195-3205.
16. Hoppel, M., et al., *Validation of the combined ATR-FTIR/tape stripping technique for monitoring the distribution of surfactants in the stratum corneum.* Int J Pharm, 2014. 472(1-2): 88-93.
17. Blaschke, T., L. Kankate, and K.D. Kramer, *Structure and dynamics of drug-carrier systems as studied by parelectric spectroscopy.* Adv Drug Deliv Rev, 2007. 59(6): 403-10.
18. Leichtnam, M.L., et al., *Identification of penetration enhancers for testosterone transdermal delivery from spray formulations.* J Control Release, 2006. 113(1): 57-62.
19. Liang, X., et al., *Folate-functionalized nanoparticles for controlled ergosta-4,6,8(14),22-tetraen-3-one delivery.* Int J Pharm, 2013. 441(1-2): 1-8.
20. Patel, N.A., N.J. Patel, and R.P. Patel, *Design and evaluation of transdermal drug delivery system for curcumin as an anti-inflammatory drug.* Drug Dev Ind Pharm, 2009. 35(2): 234-42.
21. Csizmazia, E., et al., *Ibuprofen penetration enhance by sucrose ester examined by ATR-FTIR in vivo.* Pharm Dev Technol, 2012. 17(1): 125-128.